Comparison Between Chitosan Nanoparticles and Cellulose Nanofibers as Reinforcement Fillers in Papaya Puree Films: Effects on Mechanical, Water Vapor Barrier, and Thermal Properties

Taís Téo de Barros-Alexandrino,[1,2] Milena Martelli Tosi [1,3] Odílio Benedito Garrido Assis [1]

[1]*National Nanotechnology Laboratory for Agriculture, LNNA, Embrapa Instrumentação, 13561-206, São Carlos, SP, Brazil*

[2]*PPG Biotecnology, Federal University of São Carlos, UFSCar, 13565-905, São Carlos, SP, Brazil*

[3]*Departament of Food Engineering (FZEA), University of São Paulo, USP, 13635-900, Pirassununga, SP, Brazil*

Chitosan nanoparticles (Np) were prepared by ionic gelation method, with particle size of 58.54 ± 16.99 nm. Cellulose nanofibers (Nf) were extracted from soybean straws by a combined process of mechanical grinding and enzymatic hydrolysis, with diameters between 40 and 120 nm and variable length. The puree was prepared by using overripe papayas and fillers (Np and Nf) incorporated separately at a concentration of 0.1% and 0.2% (% of filler to puree mass in dry bases) and subsequently cast into films. Mechanical characterization, both tensile strength and strain at break, were found to have significantly improved for those films reinforced with Nf. Values of tensile of 2.79 ± 1.20 MPa for chitosan and 7.30 ± 1.27 MPa for cellulose were measured for 0.2% additions. The presence of cellulose fibers (elongation of 9.33% $\pm$ 0.72%) had a greater effect on film plasticity than for chitosan Np (6.86% $\pm$ 2.17%) at 0.2% addition. About 0.2% of Nf also performed better than Np in reducing the water vapor permeation rate. Calorimetric analysis (TGA and DSC) indicated thermal stability of the composite films at temperatures above 100°C, with similar behavior between samples. POLYM. ENG. SCI., 9999:1–6, 2018. © 2018 Society of Plastics Engineers

INTRODUCTION

Films produced from fruit puree are emerging as one of the most promising avenues in the search of new biodegradable materials. Purees can be processed into continuous films, either from industrial pulps [1] or from ripe [2] and overripe [3] fruit pericarps with few technological requirements and at a low cost. Furthermore, the original color and flavor of puree-based films can be preserved, enhancing its appeal for consumption. Several fruit and vegetables, such as apple [4], mango [5], guava [6], banana [3], tomato [7], carrot [8], and papaya [9] have been tested as raw materials for filmogenic formulations. Despite offering a good oxygen barrier, the fruit puree films possess relatively high water vapor permeability (WVP) and low mechanical properties [1], which limit their broader applications.

One possible method of overcoming these drawbacks is to add reinforcement fillers into the film matrix. The formation of biocomposites by particles addition is found to be the most effective for improving both barrier and mechanical properties of biopolymer-based films [10,11]. These have been widely evaluated for films processed from fruit puree, cellulose nanofibers (Nf) [5], and chitosan nanoparticles (Np) [3] because of their strong affinity to puree compounds.

Fruit pulp generally contains a large amount of saccharides such as sugars, pectin, and cellulosic fibers bounded to polyphenolic compounds as tannins, lignins, caffeic acids, and quinones [12,13]. These contain large amounts of hydroxyl and carboxyl groups which make them polar and hydrophilic in nature and easy to form intermolecular hydrogen bonds with similar polymers.

Cellulose Nf are usually added due to their high specific strength and stiffness, resulting in improved mechanical and barrier properties. Nf are prone to form intermolecular bonds with the host matrix, including hydroxyl, glycosidic, and hemiacetal side chains linkages building multiple primary and secondary bonds and consolidating in an intricate three-dimensional network structure [14,15]. Chitosan is a polysaccharide characterized by polar groups along its chains. These favor ionic interactions predominantly by binding its amino and hydroxyl groups to the carbonyl abundant groups in the basic structure of puree matrix. The formation of conjugated imines between compounds is assumed to increase the overall structural strength [16].

Amongst those fruit and vegetables suitable for puree preparation is papaya (*Carcia papaya* L.), a popular tropical fruit that yields a large amount of pulp. Papaya is extremely perishable with a short shelf life. Due to its low calcium content the degradation of polysaccharides cell walls are accelerated, resulting in a rapid decay of texture. Estimated losses of papaya are above 40% of total production from the point of origin to the point of consumption [17,18]. Brazil is the largest producer of papaya, accounting for around 30% of world harvest [19] and therefore offers a large amount of disposed material available for puree processing.

In the present study, the feasibility of using over-ripe papaya as raw material for direct film processing is investigated, combined with the use of chitosan Np and cellulose Nf as reinforcement fillers in the composite formation.

EXPERIMENTAL

Preparation of Papaya Puree

Overripe papayas beyond stage three of maturity according to Bron and Jacomino [20] and Serry [21] classification (external

skin color 100% yellow with necrotic brown spots) were sorted, peeled, and the seeds removed. The puree was produced according to a method described elsewhere [3]. In summary, 750 g of overripe pulp (11.28 ± 1.9° Brix) was mixed in 250 g of distilled water for 3 min using a laboratory blender (Hach RO 120, USA). The puree was acidified with a combined solution of citric and ascorbic acid, both at 0.2% (wt/wt). The mixture was then centrifuged (Eppendorf 5810R, Germany), for 5 min at 12,000 rpm and the supernatant discarded. The puree was autoclaved (Phoenix, Brazil) at 115°C for 60 s for enzyme inactivation and then packaged in polyethylene bags for freezing at −20°C.

Chitosan Np

Chitosan Np were obtained by ionic gelation method [22]. Chitosan medium molar weight (400,000 g mol^{-1}) was dissolved in an aqueous solution of acetic acid at 1% (vol/vol) to a polymer concentration of 0.1% (wt/vol). Sodium tripolyphosphate (TPP) was dissolved in deionized water (pH 6.7) at the same concentration and slowly added drop by drop into chitosan solution under moderate magnetic stirring at room temperature. The formation of the Np results from interactions between TPP negative groups (OH$^-$, P$_3$O$_{10}$$^{5-}$) and chitosan positively charged amino groups (NH$_3$$^+$) [23].

The suspension was centrifuged for 30 min at 4,000 rpm and the supernatant discarded. The resultant Np were re-suspended in NaCl (1.0 mmol L^{-1}) solution. All used chemical were purchased from Aldrich Chemical Company Inc. (St. Louis, USA). The particle size distribution of the formed Np was estimated in a Zetasizer ZS 3600 (Malvern Instruments, USA) along with the polydispersity index (PDI) which ranged from 0 (monodisperse) up to 1 (complete heterodisperse). Morphological aspects were observed under FEG-SEM microscopy (JEOL JSM-6701F, Japan) by dropping a diluted solution (1/1,000) onto a silicon wafer, allowed to dry for 24 h, and then coated in carbon.

Cellulose Nf

Cellulose Nf were provided by the Chemistry Department of University of São Paulo (Ribeirão Preto, Brazil) and used as supplied. The Nf were extracted from soybean straws by a combined process of mechanical grinding and enzymatic hydrolysis, according to the process described by Martelli-Tosi et al. [24]. Fiber morphology and size was analyzed under electronic scanning microscopy (JEOL JSM-6510 SEM, Japan). The samples were fixed to aluminum stubs and coated with a thin layer of gold using a sputtering device (Balzers Union Ltd., Leichtenstein). The dimensions of fibers were determined using the freeware ImageJ (National Institutes of Health, Bethesda, MD).

Film Processing

The films were processed using a laboratory padder (Werner Mathis AG, Switzerland) running in batch mode and dried at 40°C. Formulations were prepared with a puree concentration of 15% (g of dry weight per 100 g of total solution). Chitosan Np and cellulose Nf were separately added at a proportion of 0.1 and 0.2 (g of filler per 100 g dry weight puree). About 5% of glycerol (Gly, from Synth, Brazil) was added as plasticizer and the mixtures homogenized for 15 h under moderate stirring. The formulations identification follows the relation MX_Np(Nf)Y, where MX designates the mass of puree and Y the relative proportion of

added chitosan Np or cellulose Nf respectively, as summarized in Table 1.

Mechanical Properties

Film thickness was measured using a digital hand-held micrometer (Mitutoyo Co., Kawasaki-Shi, Japan). Three values were taken at random locations along the length of each sample and the mean value used for calculation. Uniaxial tensile tests were conducted until film fracture using a Texture Analyzer TA.XT Plus (Stable Micro System, Surrey, UK), with a 50 N load cell and tensile grips at an initial separation of 80 mm. The tests were run using rectangular samples of 100 mm × 16 mm and a cross-head speed of 80 mm/min in accordance to ASTM D882-97. Stress—strain curves were plotted for each test and the ultimate stress (σ_{max}, MPa) and elongation at break (ε_{max}, %) were determined directly from the curves.

Thermal Properties

Thermogravimetric analysis (TGA) and differential scanning calorimetry (DSC) were carried out using a TGA-Q500 and DSC-Q100 equipment (TA Instruments, New Castle, USA). For TGA evaluation, samples with an initial mass of 10 mg were sealed into aluminum pans and the experiments recorded in the temperature range of 30–700°C (heating rate of 10 °C/min) under nitrogen flow at 60 mL/min. For DSC, film samples of 5 mg was accurately weighed, sealed into aluminum pans, and heated from −60 to 210°C at a heating rate of 10 °C/min.

Water Vapor Permeability

WVP was determined using an adaptation of the ASTM E96-92 gravimetric method. Distilled water (6 mL) was dispensed into flat-bottom Plexiglas cups. Circular samples were cut from each film and sealed to the cup bases achieving an effective film area of 28.27 cm^2. The cups were placed inside temperature controlled desiccators at 40°C with an internal relative humidity of 50%. The cups were weighed hourly for a period of 34 h using an analytical scale (Gehaka AG 2000, Gehaka Co., Brazil).

The water vapor transmission rate (WVT) was calculated by normalizing the slope of the linear portion of weight loss versus time to the exposed area (A_f), as described by:

$$WVT = \frac{slope}{A_f} \left(\frac{g}{m^2 s} \right)$$

And the permeability obtained as

TABLE 1. Formulation compositions for film processing[a].

Film identification	M[b] (%wt)	Np[c] (%wt)	Nf[d] (%wt)
M15	15	0	0
M15_Np0.1	15	0.1	0
M15_Np0.2	15	0.2	0
M15_Nf0.1	15	0	0.1
M15_Nf0.2	15	0	0.2

[a]All solution with 5% (wt/wt) of glycerol addition as plasticizer.
[b]Mass of papaya puree in dry basis (d.b.).
[c]Chitosan nanoparticles.
[d]Nanofibers.

$$WVP = \frac{WVT \times t}{\Delta P} \left(\frac{g}{msPa} \right)$$

where WVP is the water vapor permeability (g/ms Pa), WVT the water vapor transmission rate (g/m^2 s), t the film thickness (m), and ΔP the partial water vapor pressure difference (Pa) across the two sides of the film.

Statistical Analysis

All experiments were performed in triplicate and one-way analysis of variance (ANOVA) was performed using the Microcal Origin 9.0 software (OriginLab Co., USA).

RESULTS AND DISCUSSION

Nanofillers Characterization

The analysis of chitosan Np revealed a Gaussian bimodal distribution of sizes according to Fig. 1(a) as obtained by dynamic light scattering (zetasizer readings). A minor distribution centered at 8.9 nm and a broad one ranging from 15 to 260 nm with center at 54.3 nm were recorded. A measured polydispersity index of 0.43 indicated a system with medium heterogeneity of size and mass, similar to those previously reported [25]. The average particle size considering the pondered distribution is automatically calculated as 58.54 ± 16.99 nm. Such dimensions are consistent to those
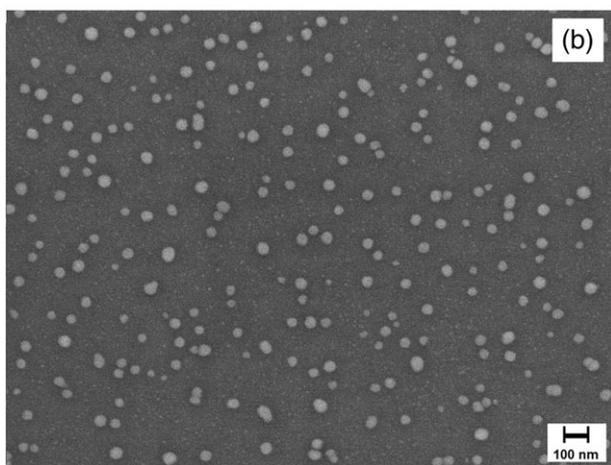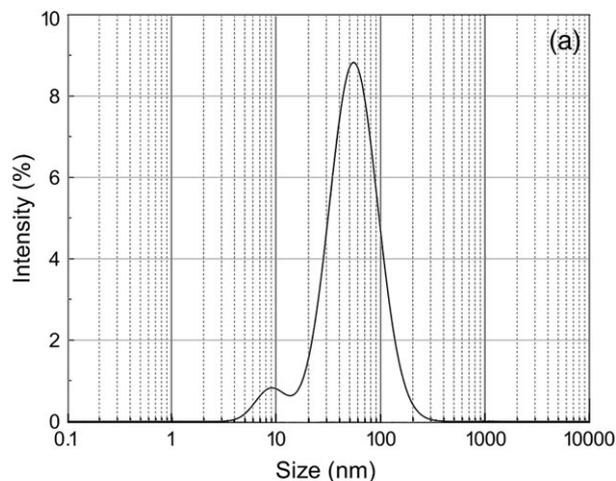
FIG. 1. Characterization of chitosan Np solution: (a) particle size distribution and (b) Np observation under FEG-SEM.
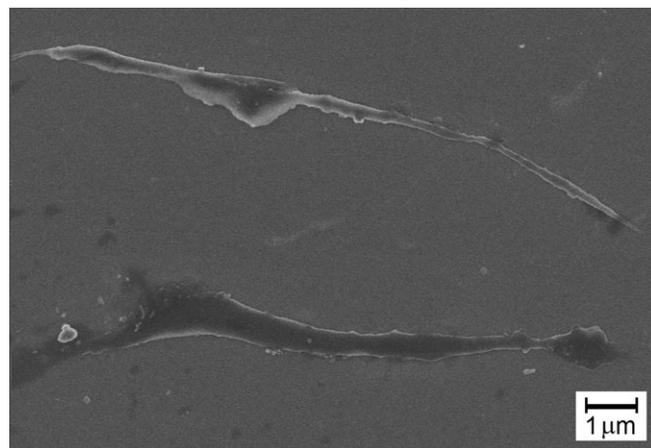
FIG. 2. FEG-SEM micrograph of cellulose Nf.

described in the literature using the ionic gelation method [26,27], and suitable for the purpose of use as reinforcement filler.

From microscopic observations (Fig. 1b), it is possible to assess the morphological aspects of the formed particles, revealing a nearly spherical shaped and dimensions conforming to those obtained by Zetasizer.

Figure 2 shows a typical microscopic aspect of isolated fibers for cellulose. In general, the resulting Nf are characterized by long cellulose micro/nanofibrils with diameter within the range 40–120 nm and variable non-uniform lengths. When in suspension the Nf tend to aggregate with each other, primarily due to hydrogen bonds between hydroxyl groups, forming a packed network of entangled fibers. The isolated fibers as well as the cluster features are very close to those presented by the method in which the process of obtaining the fibers was followed [28,29].

Mechanical Properties

Table 2 summarizes the thickness and mechanical properties of the tested films in which values of strain and tensile strength at break are expressed as a function of the relative amount of added nanofillers. The relationship between values is better visualized in graphical form as shown in Fig. 3. A concentration of 15% of puree resulted in films that were extremely brittle making them unsuitable for mechanical analysis.

The incorporation of nanofillers improved the physical film properties; however, there were alterations in the mean strain

TABLE 2. Thickness and mechanical properties of papaya puree cast films reinforced with chitosan nanoparticles and cellulose nanofibers.

Films*	Thickness (mm)	Strain, ε_{max} (%)	Tensile strength, σ_{max} (MPa)
M15	NF**	—	—
M15_Np0.1	0.169 ± 0.002	6.05 ± 1.33[b]	1.84 ± 1.60[c]
M15_Np0.2	0.182 ± 0.009	6.86 ± 2.17[a,b]	2.79 ± 1.29[c]
M15_Nf0.1	0.086 ± 0.006	7.09 ± 0.98[a,b]	6.42 ± 0.90[b]
M15_Nf0.2	0.071 ± 0.005	9.33 ± 0.72[a,b]	7.30 ± 1.27[a,b]

*Film identification according to formulation presented in Table 1.
**No formation of handled films.
Different superscript letters in the same column are statistically different (Tukey, $p < 0.05$).
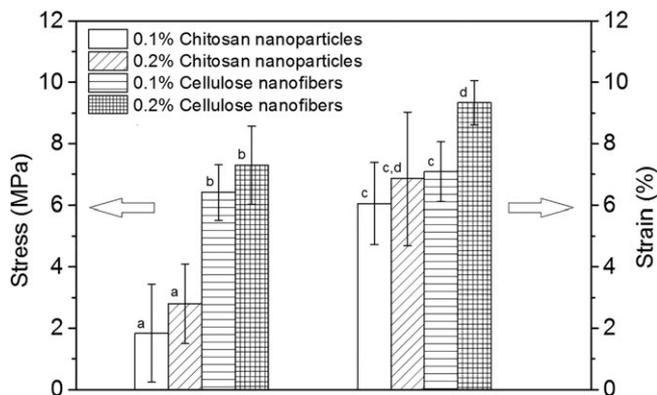
FIG. 3. Graphical comparison of film mechanical properties. Stresses and strains from different amount of added fillers. Bars with different letters are statistically different at $p < 0.05$.

(percent elongation). For a 0.2% addition of both Np and Nf, plasticity tended to increase, though with a relatively greater standard deviation. Statistically, the incorporation of reinforcement fillers is more noticeable and marked on the stress than the strain, despite of the presence of functional oxygen groups (hydroxyl and amino/acetamido for chitosan and hydroxyl and carboxyl for cellulose) that increases the affinity toward water and polar molecules adding a plasticizer effect to the matrix.

An increase in Nf content was found to result in better strength, observed as an increase in stress at break despite a reduction in the elongation. Fibers as enforcement fillers are in general more effective than circular organic Np, due to its large aspect ratio having a high surface area for interaction. In addition, fibers have a rigid nature and under optimized conditions can present an isotropic alignment. When the film is stressed the fibers will be equally strained requiring an increase in the applied stress to break down the film [30,31]. The addition of fibers resulted in thinner films compared to those with Np for a same amount of puree mass (Table 2).

Transmission microscopy analysis has revealed that both chitosan Np and cellulose Nf can be properly dispersed and bonded into the polymeric matrix, forming strong interactions due to chemical similarities [30,32]. The reinforced samples present average elongations similar to those reported by Lorevice et al. [33] when assessing papaya puree films with chitosan Np associated to hydroxypropyl methylcellulose. The tensile strengths are not far from the values measured by Otoni et al. [9] for papaya/pectin films with nanoemulsions of cinnamaldehyde. In general, the mechanical properties are similar to literature data. Fibers incorporation into polysaccharides films introduces a comparatively higher effect than Np on overall mechanical properties [34]. This has been attributed to the higher density of [sbond] OH groups on the cellulose surface favoring the bonding to hydroxyl groups of the surrounding matrix [28].

Thermal Characterization

Figure 4 shows the TG curves of the puree and reinforced films according to the classification shown in Table 1. All samples follow a similar pattern with continuous weight loss in one initial dehydration step (removal of moisture and volatile materials) in an interval of around 180 to 210°C (T_1) followed by decomposition. According to the DTG curve corresponding to the derivative
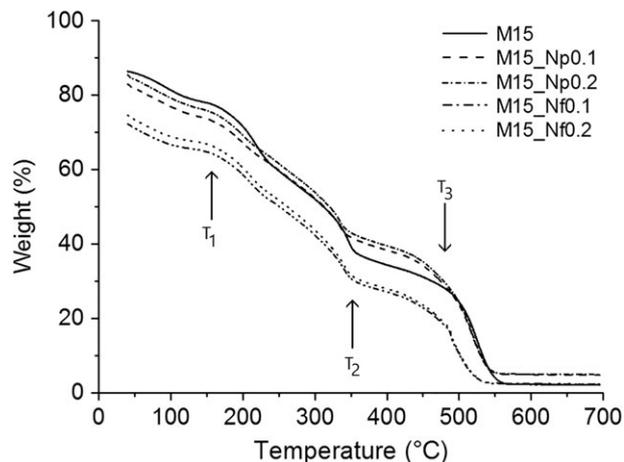
FIG. 4. TG curves for M15 (15% d.b.) series films with reinforcement fillers (heating hate: 10 °C/min). The arrows indicate the temperature region of the main thermal decomposition.

TG (not shown), at least two more events are identifiable. One of these is at around 350°C (T_2) and is related to thermal irreversible degradation of sugars (fructose, glucose, and sucrose), starch, and proteins. A second is observed at approximately 480°C (T_3) and may be attributed to the carbonation of the degraded organic compounds (lignin, hemicellulose, and cellulose). The percentages of residual mass in each of these stages are numerically displayed in Table 3.

The 0.2% content of nanofillers resulted in a proportionally higher loss of mass in the dehydration event than that measured for 0.1% addition. Such a result is due to the hydrophilic nature of the fillers, particularly cellulose which absorbs a greater amount of water and therefore exhibits a higher dehydrated volume (expressed by the residual mass at T_1). The presence of a higher volume of water for 0.2% of fillers is also apparent by an improvement in mechanical properties, the films exhibiting a better plasticity attributed to the water plasticizing effect.

It is noted that the incorporation of chitosan Np results in the highest mass losses in all thermal events. The Np ability to be distributed and incorporated into the matrix raises the structural strength, resulting in a reduction in thermal instability which is consistent with previously reported studies [3,35].

The DSC curves are shown in Fig. 5. The sub-zero glass transition temperature is measured to be around −30°C for neat puree, close to that measured for puree films processed from other fruits [3,5]. According to Azeredo et al. [5], such a low temperature

TABLE 3. Percentage of residual mass according to thermal parameters from TGA curves.

Films	T_1 (%)	T_2 (%)	T_3 (%)	RM (%)
M15	76	37	28	2
M15_Np0.1	75	43	25	5
M15_Np0.2	72	41	26	5
M15_Nf0.1	68	30	19	2
M15_Nf0.2	64	29	19	2

T_1 = % of mass after the first event (dehydration); T_2 = % of mass after the second event (sugar decomposition); T_3 = % of mass after the third event (organic compounds degradation); RM = % of mass after the thermal cycle (residual mass at 700°C).
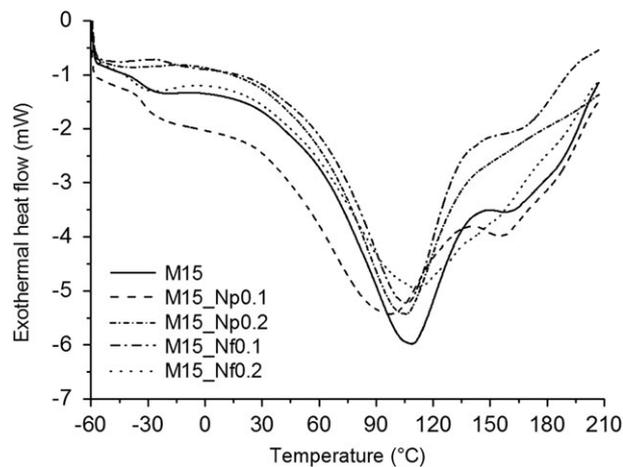
FIG. 5. DSC scans of papaya puree films (15% d.b.) with reinforcement fillers.

FIG. 6. WVP as a function of filler type and content. Bars with different letters are statistically different at $p < 0.05$.

reflects poor chemical stability of the matrix resulting from elevated molecular mobility and consequently high reactivity of its compounds.

The incorporation of cellulose Nf appeared not to alter the T_g of the puree films, an effect that is clearly observed when chitosan Np are added (Table 4). Cellulose fibers have a natural tendency to agglomerate [29] and if not well dispersed can result in irregular distribution which reduces the amount of interactions. The Np, however, assume a more homogeneous distribution resulting in efficient crosslinking points with the matrix compounds [6]. Consequently, the mobility of chain segments can be reduced, reflecting an increase in measured glass transition temperature.

The stabilizing effect of chitosan Np is also confirmed by an increase in temperature of the second endothermic event (degradation of cellulosic basic compounds) and the corresponding enthalpy (heat absorbed per unit weight of film sample). This reveals the effect of partial crystallinity, where fractions are proportionally larger when the fillers are incorporated.

Water Vapor Permeability

The papaya control film (M15) has permeability comparable to values reported to peach [1], banana [3], and mango [5] films processed and essayed in similar conditions. The WVP values are shown in Fig. 6 as function of filler type and concentration and confirm a reduction in water permeation through the papaya matrix.

The cellulose Nf proved to be more effective in decreasing the permeability even for thinner films (Table 2), showing a reduction superior to 60% (from 3.50 to 1.38 g mm/m^2 h kPa) for 0.2% addition (M15_Nf0.2). This improvement in the barrier properties

may be attributed to an increase in the tortuosity of the diffusive path for penetrant molecules [36], induced mainly by the higher aspect ratio of the fibers.

Although the chitosan Np have also an effect on WVP, their incorporation resulted in comparatively smaller interference. This is somewhat expected since the circular format and particle dimensions are prone to more regular distribution, thus not impacting significantly on the tortuosity of the matrix. It should be noted that in analysis conducted by de Moura et al. [36], it was shown that the size of chitosan Np had an important effect on the reduction of WVP in organic films. Small size Np act better, since they are more able to access empty spaces thus hindering the diffusion of water throughout the film.

CONCLUSIONS

Cellulose Nf and chitosans Np at concentrations of 0.1 and 0.2% (db) were used as reinforcing filler in papaya puree based films. The fillers improved handling of the papaya films yielding measurable improvements on both mechanical and water vapor barrier properties. Overall, Nf were more effective in increasing tensile strength and strain at break than chitosan Np for similar concentrations. The water vapor barrier properties were also improved, particularly when 0.2% of cellulose Nf were incorporated into the matrix. All samples showed similar thermal behavior, although the influence of chitosan Np had a more pronounced effect in increasing the T_g, enthalpy and final residual mass at 700°C, resulting in an increase in film structural stability.

TABLE 4. Thermal parameters from DSC curves.

Films	T_g (°C)	Endothermic main peak (°C)	Endothermic secondary peak (°C)	ΔH (J g^{-1})
M15	−30.09	107.92	161.52	136
M15_Np0.1	−22.92	105.71	170.45	167
M15_Np0.2	−13.01	104.31	—	145
M15_Nf0.1	−29.62	94.75	156.89	123
M15_Nf0.2	−30.75	108.57	—	146

REFERENCES

1. T.H. McHugh, C.C. Huxsoll, and J.M. Krochta, *J. Food Sci.*, **61** 88 (1996).
2. R. Sothornvit and P. Rodsamran, *Postharvest Biol. Technol.*, **47** 407 (2008).
3. M.R. Martelli, T.T. Barros, M.R. Moura, L.H.C. Mattoso, and O. B.G. Assis, *J. Food Sci.*, **78** N98 (2013).
4. W.-X. Du, C.W. Olsen, R.J. Avena-Bustillos, T.H. McHugh, C. E. Levin, and M. Friedman, *J. Agric. Food Chem.*, **56** 3082 (2008).

5. H.M.C. Azeredo, L.H.C. Mattoso, D. Wood, T.G. Williams, R. J. Avena-Bustillos, and T.H. McHugh, *J. Food Sci.*, **74** N31 (2009).

6. M.V. Lorevice, M.R. Moura, F.A. Aouada, and L.H.C. Mattoso, *J. Nanosci. Nanotechnol.*, **11** 1 (2012).

7. W.-X. Du, C.W. Olsen, R.J. Avena-Bustillos, T.H. McHugh, C. E. Levin, and M. Friedman, *J. Food Sci.*, **73** M375 (2008).

8. X. Wang, X. Sun, H. Liu, M. Li, and Z. Ma, *Food Bioprod. Process.*, **89** 149 (2011).

9. C.G. Otoni, M.R. Moura, F.A. Aouada, G.P. Camilloto, R. S. Cruz, M.V. Lorevice, N.F.F. Soares, and L.H.C. Mattoso, *Food Hydrocolloids*, **41** 188 (2014).

10. F. Chivrac, E. Pollet, and L. Avérous, *Mater. Sci. Eng. R: Rep.*, **67** 1 (2009).

11. H. Ku, H. Wang, N. Pattarachaiyakoop, and M. Trada, *Compos. Part B: Eng.*, **42** 856 (2011).

12. N. Rispail, P. Morris, and K. Webb. "Phenolic Compounds: Extraction and Analysis," in Lotus Japonicus Handbook, , A. Márquez, Ed. Berlin, Springer 349 (2005).

13. C.W.I. Haminiuk, G.M. Maciel, M.S.V. Plata-Oviedo, and R. M. Peralta, *Int. J. Food Sci. Technol.*, **N47** 2023 (2012).

14. A.K. Bledzki, S. Reihmane, and J. Gassan, *Polym. Plast. Technol.*, **37** 451 (1998).

15. H. Habibi, A.A. Lucia, and O.J. Rojas, *Chem. Rev.*, **110** 3479 (2010).

16. J.M. Urreaga and M.U. de la Orden, *Eur. Polym. J.*, **42** 2606 (2006).

17. J.A. Teixeira, S. Zinia, R. Duong, T. Nhut, D. Sivakumar, A. Gera, M. Teixeira, and P.F. Tennant, *Tree Forest. Sci. Biotechnol.*, **1** 47 (2007).

18. J.C. Buzby, J.T. Bentley, B. Padera, C. Ammon, and J. Campuzano, *Agriculture*, **5** 626 (2015).

19. L.C. Costa, W.S. Ribeiro, E.I.B. Almeida, G.G. Carneiro, and J. A. Barbosa, *Rev. Agropec. Téc.*, **32** 21 (2011) In portuguese.

20. I.U. Bron and A.P. Jacomino, *Braz. J. Plant Physiol.*, **18** 389 (2006).

21. N.K.H. Serry, *Am.-Eurasian J. Agric. Environ. Sci.*, **11** 205 (2011).

22. P. Calvo, C. Remuñán-López, J.L. Vila-Jato, and M.J. Alonso, *J. Appl. Polym. Sci.*, **63** 125 (1997).

23. S. Kunjachan and S. Jose, *Asian J. Pharm.*, **4** 148 (2010).

24. M. Martelli-Tosi, M. d. S. Torricillas, M. A. Martins, O.B.G. d. Assis, and D.R. Tapia-Blácido, *J. Nanomater*, **2016** 1–10 (2016).

25. L. Pilon, P.C. Spricigo, M. Miranda, M.R. de Moura, O.B. G. Assis, L.H.C. Mattoso, and M.D. Ferreira, *Int. J. Food Sci. Technol*, **50** 440 (2015).

26. T. López-León, E.L.S. Carvalho, B. Seijo, J.L. Ortega-Vinuesa, and D. Bastos-González, *J. Colloid Interface Sci.*, **283** 344 (2005).

27. A. Nasti, N.M. Zaki, P. de Leonardis, S. Ungphaiboon, P. Sansongsak, M.G. Rimoli, and N. Tirelli, *Pharm. Res.*, **26** 1918 (2009).

28. B. Wang and M. Sain, *Polym. Int.*, **56** 538 (2007).

29. M. Martelli-Tosi, O.B.G. Assis, N.C. Silva, B.S. Esposto, M. A. Martins, and D.R. Tapia-Blácido, *Carbohyd. Polym.*, **157** 512 (2017).

30. P.R. Chang, R. Jian, J. Yu, and X. Ma, *Food Chem.*, **120** 736 (2010).

31. M. Pereda, G. Amica, I. Rácz, and N.E. Marcovich, *J. Food Eng.*, **103** 76 (2011).

32. T. Zimmermann, N. Bordeanu, and E. Strub, *Carborydr. Polym.*, **79** 1086 (2010).

33. M.V. Lorevice, M.R. Moura, and L.H.C. Mattoso, *Quím. Nova*, **37** 931 (2014) In portuguese.

34. A. Dusfresne and J. Castaño, *Starch/Stärke*, **69** 1500307 (2017).

35. M. Abdollahi, M. Alboofetileh, M. Rezaei, and R. Behrooz, *Food Hydrocolloids*, **32** 416 (2013).

36. M.R. de Moura, F.A. Aouada, R.J. Avena-Bustillos, T. H. McHugh, J.M. Krochta, and L.H.C. Mattoso, *J. Food Eng.*, **92** 448 (2009).